Functional solubilisation of the β_2-adrenoceptor (β_2AR) using Diisobutylene maleic acid (DIBMA)

C. R. Harwood[1,2], D. A. Sykes[1,2], B. Hoare[1,2], F. M. Heydenreich[3,#] R. Uddin[2,4], D. R. Poyner[2,4], S. J. Briddon[1,2,*], D. B. Veprintsev[1,2,*]

[1]Division of Physiology, Pharmacology and Neuroscience, School of Life Sciences, Queen's Medical Centre, University of Nottingham, Nottingham NG7 2UH, UK
[2]Centre of Membrane Proteins and Receptors (COMPARE), University of Birmingham and University of Nottingham, Midlands NG7 2UH, UK
[3]Laboratory of Biomolecular Research, Paul Scherrer Institute, 5232 Villigen PSI, Switzerland and Department of Biology, ETH Zürich, 8093 Zürich, Switzerland
[4]School of Life and Health Sciences, Aston University, Birmingham B47ET, U.K
[#]current address: Department of Molecular and Cellular Physiology, Stanford University School of Medicine, Stanford, CA 94305, USA
*correspondence should be addressed to stephen.briddon@nottingham.ac.uk and dmitry.veprintsev@nottingham.ac.uk

Abstract

The β2-adrenoceptor (β2AR) is a well-established target in asthma and a prototypical GPCR for biophysical studies. Solubilisation of membrane proteins has classically involved the use of detergents. However, the detergent environment differs from the native membrane environment and often destabilises membrane proteins. Use of amphiphilic copolymers is a promising strategy to solubilise membrane proteins within their native lipid environment in the complete absence of detergents. Here we show the isolation of the β_2AR in the polymer Diisobutylene maleic acid (DIBMA). We demonstrate that β_2AR remains functional in the DIBMA lipid particle (DIBMALP) and shows improved thermal stability compared to the n-Dodecyl-β-D-Maltopyranoside (DDM) detergent solubilised β_2AR. This unique method of extracting β_2AR offers significant advantages over previous methods routinely employed such as the introduction of thermostabilising mutations and the use of detergents, particularly for functional biophysical studies.

Introduction

G protein coupled receptors (GPCRs) are the largest family of membrane proteins within the human genome and are responsible for modulating a broad range of hormonal, neurological and immune responses. It is well established that GPCRs have a large therapeutic potential. Indeed, GPCRs currently represent 34% of all US food and drug administration (FDA) approved drugs, with 475 drugs targeting over 100 diverse receptors (Hauser, Attwood et al. 2017). The β_2-adrenoceptor (β_2AR) is a rhodopsin-like family GPCR (Schioth and Fredriksson 2005) and member of the adrenoceptor family, which signals primarily through coupling the heterotrimeric G_s protein. It is a well-established target for asthma and has become one of the most studied GPCRs with several structural (Wacker, Fenalti et al. 2010, Rasmussen, DeVree et al. 2011, Bang and Choi 2015) and detailed biophysical studies (Manglik, Kim et al. 2015, Gregorio, Masureel et al. 2017) into its activation mechanism.

A prerequisite for completion of biophysical and structural studies is the extraction and isolation of the β_2AR from its cellular environment. Classically, this has involved the use of detergents, in the case of the β_2AR and other GPCRs, *n*-dodecyl-β-D-maltopyranoside (DDM) is most often used (Munk, Mutt et al. 2019). However, it is well established that detergent micelles do not recapitulate the environment of the cell membrane and, as such, protein stability is compromised. Moreover, there is strong evidence that phospholipid composition affects β_2AR function (Dawaliby, Trubbia et al. 2016). Cholesterol in particular appears associated with the β_2AR in crystal structures (Cherezov, Rosenbaum et al. 2007), and improves β_2AR stability (Zocher, Zhang et al. 2012) and function (Paila, Jindal et al. 2011). Multiple studies (Leitz, Bayburt et al. 2006)(Whorton, Bokoch et al. 2007) have mimicked the native membrane environment and improved protein stability through reconstitution of membrane proteins in liposomes, amphipols or synthetic nanodiscs, however these all require initial use of detergents to extract the membrane protein from the membrane.

Recently, it was discovered that styrene maleic acid (SMA) copolymer directly incorporates into biological membranes and self-assembles into native nanoparticles, known as Styrene Maleic Acid Lipid Particles (SMALPs) (Knowles, Finka et al. 2009) (Stroud, Hall et al. 2018). This has provided a novel method for the solubilisation of membrane proteins with their native receptor associated phospholipids, whilst avoiding the use of detergents at all stages. SMA has been used to solubilise a range of membrane proteins (Dorr, Koorengevel et al. 2014, Gulati, Jamshad et al. 2014, Sun, Benlekbir et al. 2018) including GPCRs (Bada Juarez, Munoz-Garcia et al. 2020)(Jamshad, Charlton et al. 2015) for both structural and biophysical studies. Such studies either improved protein stability compared to detergent or have allowed extraction of membrane proteins that were previously unstable in detergents. There is, however, evidence that the conformational flexibility of GPCRs within SMALPs is restricted (Mosslehy, Voskoboynikova et al. 2019)(Routledge, Jamshad et al. 2020) therefore differing from the native state of the protein. Furthermore, the high absorbance of SMA copolymer in the far-UV region makes optical spectroscopic studies of membrane proteins that are encapsulated within SMALPs challenging, and SMALPs are known to be disrupted by divalent cations (Gulamhussein, Meah et al. 2019).

An alternative to SMA is Diisobutylene maleic acid (DIBMA), a copolymer which was developed specifically for the extraction of membrane proteins from the intact bilayer (Oluwole, Klingler et al. 2017). Compared to SMALPs, DIBMALPs are believed to have only a mild effect on lipid packing, be compatible with optical spectroscopy in the far UV range, and tolerate low millimolar concentrations of divalent cations (Oluwole, Klingler et al. 2017). This makes DIBMALPs far more amenable for functional biophysical studies. Although the disk size of SMALPs is believed to vary with different ratios of styrene to maleic acid, DIBMALPs are generally thought to have a larger hydrodynamic radius than SMALPs (Oluwole, Danielczak et al. 2017).

In this study we demonstrate isolation of the functional β_2AR from the mammalian cell membrane using DIBMA, with improved thermal stability compared to conventional detergent based methods.

Results

DIBMALP-β_2AR retains its pharmacology

A time-resolved fluorescence resonance energy transfer (TR-FRET) based ligand binding assay was established to investigate if the β_2AR remained functional when extracted from the HEK cell membranes into DIBMALPs. Figure **1** shows saturation binding experiments for the fluorescent antagonist *S*-propranolol-red-630/650 (F-propranolol) (Hello Bio, UK) binding membrane-β_2AR, DDM-β_2AR and DIBMALP-β_2AR. The β_2AR retained ligand binding ability when extracted from the membrane using both DDM and using the copolymer DIBMA. These data showed comparable affinities for F-propranolol binding to the β_2AR in membranes (pK_d = 7.50 ± 0.05), DDM (pK_d = 7.10 ± 0.08) and DIBMA pK_d = 7.00 ± 0.13), although with slightly reduced affinity in DIBMA compared to membranes (P=0.02, one-way ANOVA and Tukey's multiple comparison).

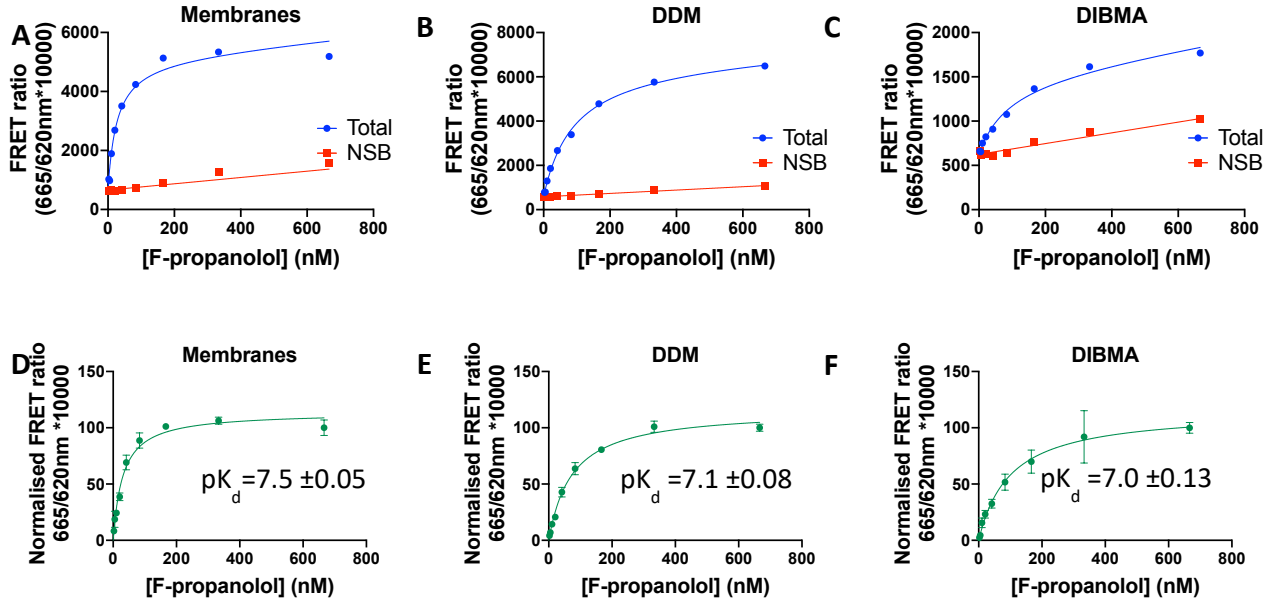

Figure 1: A comparision of F-propranolol binding to β_2AR in membranes, DDM and DIBMALPs. A-C) Representative F-propranolol (2-666nM) equilibrium saturation plots showing total and non-specific binding to the β_2AR in (A) HEK cell membranes, (B) DDM and (C) DIBMALPs, n=1. **D-F)** Saturation binding curves showing specific binding and associated affinity (pK_d) values for F-propranolol binding to the β_2AR in (D) HEK cell membranes, (E) DDM and (F) DIBMALPs, curves show combined normalised data mean ± SEM, n=3.

In order to better understand if the conformational state of the receptor or its ability to adopt different states in DIBMALPs was affected we investigated its pharmacology using the full agonist isoprenaline, the antagonist propranolol and the inverse agonist ICI 118,551 in equilibrium competition binding assays using F-propranolol as the tracer (Figure **2**). Increasing concentrations of each competing ligand produced a reduction in the specific binding of F-propranolol to the β_2AR in membranes, DDM and DIBMALPs with largely comparable pK_i values (Table **1**). The only statistically significant difference was between isoprenaline binding to the β_2AR found in

membranes versus the DDM solubilised β_2AR (p=0.03) (one-way ANOVA and Tukey's post hoc). The slopes of all curves were similar to 1.

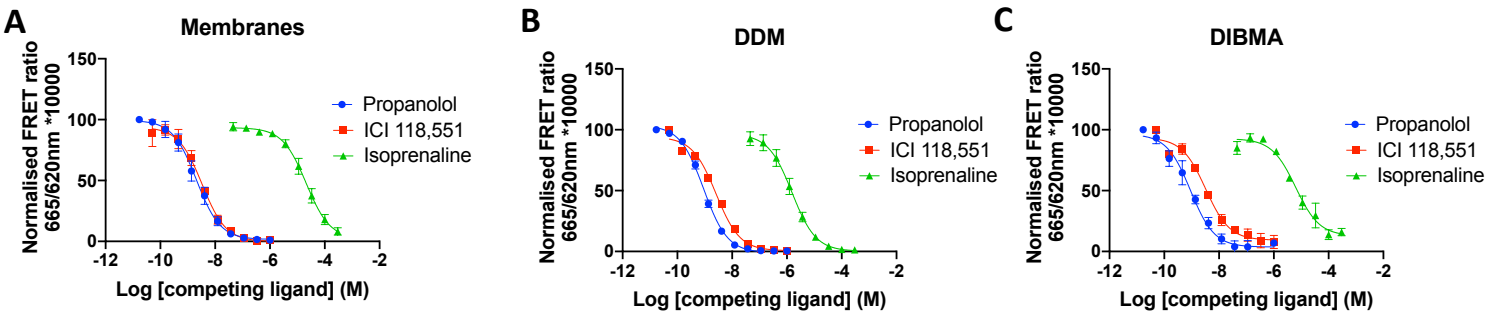

Figure 2: Competition TR-FRET ligand binding studies using F-propranolol as a tracer and unlabelled propranolol, ICI 118,551 and isoprenaline as competitors. **A)** β_2AR membranes, **B)** DDM-β_2AR **C)** DIBMALP- β_2AR, curves show normalized combined data of n=3, error bars show ± SEM.

Table 1: **A summary of pIC_{50}, pK_i and Hill slope values for propranolol, ICI 118,551, and isoprenaline obtained through TR-FRET competition binding assays. Values show mean of n=3 individually fitted curves ±SEM.**

	Membranes			DDM			DIBMA		
	pIC_{50}	**pK_i**	**Slope**	**pIC_{50}**	**pK_i**	**Slope**	**pIC_{50}**	**pK_i**	**Slope**
Propranolol	8.7 ±0.13	9.5 ±0.03	1.0 ±0.02	9.0 ±0.04	9.5 ±0.03	1.2 ±0.04	9.1 ±0.10	9.6 ±0.10	0.8 ±0.30
ICI 118,551	8.5 ±0.10	9.3 ±0.15	1.1 ±0.22	8.5 ±0.02	8.9 ±0.10	1.0 ±0.06	8.3 ±0.15	9.1 ±0.06	1.3 ±0.23
Isoprenaline	4.7 ±0.12	5.5 ±0.20	1.1 ±0.11	5.8 ±0.06	6.3 ±0.13	1.1 ±0.09	5.1 ±0.18	5.8 ±0.10	1.1 ±0.15

DIBMALP-β_2AR shows improved stability

Next, we investigated the thermostability of the DIBMALP-β_2AR using a novel ThermoFRET assay (Figure **3**). Labelling of the SNAP tag on the N terminus of the receptor with Lumi4-Tb allowed thermostability to be investigated without purifying the receptor. β_2AR unfolding was initially measured by quantifying TR-FRET between Lumi4-Tb and BODIPY™ FL L-Cystine that covalently reacts with cysteines which become exposed as the receptor unfolded (Tippett et al, in preparation).

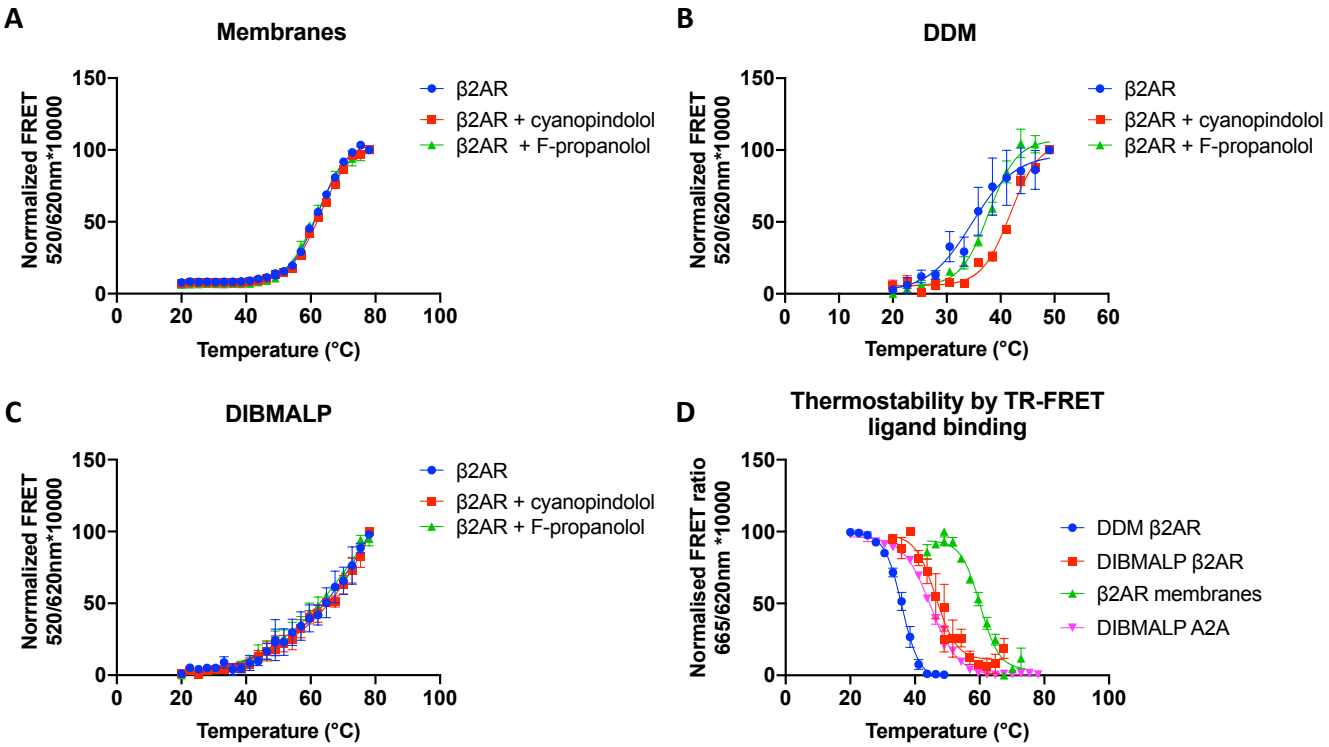

Figure 3: ThermoFRET thermostability curves in **A)** β_2AR membranes **B)** DDM solubilised β_2AR **C)** DIBMALP-β_2AR in the presence and absence of cyanopindolol (100μM) and F-propranolol (200nM). **D)** β_2AR and A_2AR TR-FRET thermostability curves obtained by measuring reduction in fluorescent F-propranolol (200nM) and F-XAC (200nM) binding. All curves show normalized combined data, data points show mean ± SEM, for n=3.

Table 2. **A summary of mean melting temperature (Tm) values ± SEM for β_2AR in mammalian cell membranes, DDM detergent micelles or DIBMALPs with or without F-propranolol, or cynapindolol measured by HTRF using ThermoFRET or binding of fluorescent ligand F-propranolol as the probe. DIBMALP-A_{2A} thermostability was measured using F-XAC.**

	Tm (°C) ThermoFRET	Tm(°C) F-ligand
Membrane β_2AR	62.4±0.2	-
Membrane β_2AR + F-propranolol	61.6±0.4	60.1±0.6 °C
Membrane β_2AR + cyanopindolol	63.0±0.4	-
DDM β_2AR	35.2±2.4	-
DDM β_2AR + F-propranolol	37.8 ±0.4	36.0 ±0.6
DDM β_2AR + cyanopindolol	41.9 ±0.1	-
DIBMALP β_2AR	-	46.8 ±2.1
DIBMALP A_{2A} + F-XAC	-	44.8 ±0.7

Figure **3B** shows the Tm of DDM solubilised β_2AR as 35.2±2.4 °C. Ligand-induced shifts in thermostability were seen when the DDM solubilised β_2AR was incubated with F-propranolol (Tm=37.8±0.4°C, p>0.05) and cyanopindolol (41.9 ±0.1 °C, p=0.04) (one-way ANOVA and Tukey's multiple comparison test). Figure **3A** shows the Tm of β_2AR in the membrane environment as 62.42±0.2°C. No ligand induced shift was observed when β_2AR membranes were pre-incubated with F-propranolol or cyanopindolol, this suggests the unfolding of the receptor itself is not directly measurable and perhaps that these data show the disintegration of the membrane itself. Figure **3C** shows TR-FRET thermostability data for the DIBMALP-β_2AR, this data did not fit a Boltzmann sigmoidal curve as the top end of the temperature range did not plateau. No effect on any part of the curve was observed with the addition of F-propranolol or cyanopindolol. Therefore, as was the case in membranes, the observed thermostability changes in DIBMALPs likely reflect the melting of the lipid particles as opposed to the receptor itself.

We then investigated the thermostability of the β_2AR by measuring the reduction in TR-FRET binding of F-propranolol over an increasing temperature range (Figure **3D**). The resulting data suggests similar Tm values determined for the membrane-β_2AR (60.1±0.6 °C) and DDM-β_2AR (36.0±0.6 °C) to those obtained using BODIPY™ FL L-Cystine in the presence of F-propranolol. Unpaired two-tailed t tests showed no statistically significant differences between membrane-β_2AR and DDM-β_2AR Tm values obtained with F-propranolol measured using either TR-FRET method.

Thermostability of DIBMALP-β_2AR measured by the decrease in F-propranolol binding gave a curve that could be fitted to a Boltzmann with a Tm value of 46.8 ± 2.1 °C. This Tm value is statistically significant from that of membrane-β_2AR (p=0.0002) and DDM-β_2AR (p=0.0009) obtained by the same method (one-way ANOVA and Tukey's multiple comparison test). Therefore, the DIBMALP-β_2AR shows approximately 10°C improved stability over the conventional DDM-β_2AR. We also observed differences in the slopes of DIBMALP-β_2AR and DDM-β_2AR thermostability curves obtained by this method, these were -3.2 and -2.7 respectively. Additionally,

we investigated the thermostability of another rhodopsin-like GPCR, the adenosine 2A receptor ($A_{2A}R$) when solubilised into a DIBMALP using fluorescent adenosine receptor antagonist (F-XAC) (Hello Bio, UK). Measuring the reduction in F-XAC bound to $A_{2A}R$ over an increased temperature range gave a Tm value of 44.8^{o}C±0.7, which was not statistically significantly different from that of the DIBMALP-β_2AR.

Discussion

The β_2AR has become the prototypical GPCR for understanding GPCR structure and the molecular basis of signaling (Bang and Choi 2015) (Gregorio, Masureel et al. 2017), these studies have all required the use of detergents to extract the β_2AR from the plasma membrane. Detergents do not recapitulate the complexity of the native membrane environment and are known to damage membrane proteins. Here, we demonstrate that the polymer DIBMA can be used to extract the β_2AR from the plasma membrane, together with its native phospholipids, avoiding the use of detergents at any stage.

We used TR-FRET ligand binding studies to show that the β_2AR remained functional inside the DIBMALP (Figure **2-3**). Ligand binding data showed comparable affinity (pK_d/K_i) values for the β_2AR binding F-propranolol, propranolol, ICI 118,551 and isoprenaline solubilised in DIBMA compared to membranes. Although the difference in pK_d values for F-propranolol binding membranes-β_2AR (7.5±0.05) and DIBMALP-β_2AR (7.0±0.13) was statistically different (P=0.02), this is only a 3 fold difference and the pharmacological importance of this remains to be seen. There was no statistical difference between F-propranolol pK_d values for DDM-β_2AR and DIBMALP- β_2AR. All ligand binding curves showed one phase binding and a slope of 1 indicating no co-operativity of ligand binding.

While the pK_d values for different preparations of the receptor were comparable, the signal amplitude obtained for F-propranolol binding DIBMALP-β_2AR in TR-FRET experiments was 3-fold lower than for membranes-β_2AR. This reduction in signal amplitude could be due to an effect of the DIBMA polymer on the TR-FRET, for example fluorescence quenching. Alternatively, it could reflect a lower fraction of the ligand binding capable β_2AR receptors present compared to the amount of Tb3+ labelled receptor molecules. However, it should be noted that the assay window for DDM-β_2AR was higher than that of membranes whilst it would be expected that less β_2AR is functional, suggesting that the solubilization environment can influence the observed signal amplitude. Whilst the concentration of β_2AR used in each experimental condition was quantified using 620nm emission of Lumi4-Tb, it was not possible to account for difference in Lumi4-Tb quantum yield in the membrane, DDM and DIBMALP environments.

It has been shown that the conformational changes of another class A GPCR, Rhodopsin II in response to activation by light are restricted in SMALPs (Mosslehy, Voskoboynikova et al. 2019). We chose to study the binding of a full agonist (isoprenaline), antagonist (propranolol) and inverse agonist (ICI 118,551) to be able to ascertain if conformational states of the β_2AR differed in a membrane, DDM micelle, or DIBMALP environment. A substantial increase or decrease in pK_i value would demonstrate an increase or decrease in the population of the receptors in the conformational state stabilized by the ligand, and therefore a difference in the conformational landscape of the receptor. As there was no statistically significant difference in pK_i values between membrane-β_2AR and DIBMALP-β_2AR it can be concluded that the DIBMALP-β_2AR represents the native conformational landscape of the β_2AR. The difference in pK_i value between DDM-β_2AR (6.3±0.13) and membrane-β_2AR (5.5±0.2) for isoprenaline was statistically significant (p=0.03), this may indicate a change in the conformational state of β_2AR in the DDM micelle compared to its native conformational state. Propranolol, ICI 118,551 and isoprenaline pK_i values obtained

in this study are in line with the previous studies that investigate the affinity of these compounds for the β_2AR (Baker 2005) (Sykes, Parry et al. 2014).

Furthermore, we employed a ThermoFRET based thermostability assay to investigate the stability of the DIBMALP-β_2AR compared to the DDM-β_2AR**.** We show the thermostability of DIBMALP-β_2AR is 10^{o}C higher than that of the DDM-β_2AR**.** It was not possible to find any thermostability data for the β_2AR in synthetic nanodiscs; however, the only other method to show a similar (11^{o}C) increase in thermostability for β_2AR is that of thermostabilizing mutations (Serrano-Vega and Tate 2009). Since these mutations also lead to a shift in the β_2AR's conformational landscape to the antagonist-bound and inactive form, the DIBMALP-β_2AR offers a clear advantage for study of receptor function.

Moreover, thermostability data for DIBMALP-β_2AR using F-propranolol showed a Tm value that was very similar to the Tm of DIBMALP-A_{2A}R. In addition, no shift in thermostability was observed for DIBMALP-β_2AR preincubated with F-propranolol or the high-affinity antagonist cyanopindolol. It therefore seems likely that this Tm value of ~45^{o}C for DIBMALP-β_2AR corresponds to the melting temperature of the DIBMALP. A Tm of 60.2 ± 0.2^{o}C seen for β_2AR in membranes was also unaffected by the presence of F-propranolol and cyanopindolol. As this Tm of 60.2^{o}C ±0.2 is statistically significant from that of the DIBMALPs it seems likely that the Tm of ~45^{o}C corresponds to disruption of the protein-lipid-polymer particles, whilst the Tm of 60.2 ±0.2^{o}C corresponds to the melting or disruption of the membrane itself. We also noted a shallower slope for DIBMALP-β_2AR (-3.2) compared to DDM-β_2AR (-2.7), this broader transition may reflect the more heterogenous nature of DIBMALPs compared to the detergent micelle.

In summary, here we show the utility of the copolymer DIBMA to solubilise the functional β_2AR. We show that this method offers improved stability over the use of the conventional detergent DDM and has allowed us to maintain the native environment and pharmacological activity of the β_2AR.

Author contributions

C.R.H performed the experiments.
C.R.H. wrote the manuscript and it was edited by, **D.A.S, D.R.P**, **S.J.B** and **D.B.V**
D.A.S gave technical advice and generated reagents.
R.U and **D.R.P** gave technical advice.
B.H and F.M.H. generated reagents.
C.R.H, S.J.B and D.B.V conceived the idea.
S.J.B and D.B.V supervised the project

Acknowledgements

This work was funded by a Medical Research Council (MRC) PhD studentship to C.R.H.

Declaration of interests

The authors declare no conflict of interest.

Supplementary information

Methods

Molecular biology

The construct pcDNA4TO-TwinStrep(TS)-SNAP-β_2AR was generated by amplification of the SNAP and β_2AR sequences of the pSNAPf-ADRB2 plasmid (NEB) and insertion into pcDNA4TO-TS using Gibson assembly (Heydenreich, Miljus et al. 2017). The construct pcDNA4TO-TS-SNAP-A_{2A} was generated by amplifying the A_{2A} receptor from the pDNA3.1 SNAP A_{2A} construct described in (Comeo, Kindon et al. 2020) and inserting into pcDNA4TO-TS-SNAP vector using Gibson assembly. This therefore gave the construct pcDNA4TO-TS-SNAP-$A_{2A.}$ Both constructs used a signal peptide based on the $5HT_{3A}$ receptor to increase protein folding and expression.

Transfection and mammalian cell culture

pcDNA4TO-TS-SNAP-β_2AR or pcDNA4TO-TS-SNAP-A_{2A} were stably transfected into T-Rex^{TM}-293 cells (Invitrogen) using polyethylenimine (PEI). A mixed population stable line was selected by resistance to 5 µg/mL blasticidin and 20 µg/mL Zeocin. Stable cell lines were maintained in high glucose DMEM (Sigma D6429) with 10% foetal bovine serum (FBS), 5µg/µL blasticidin and 20µg/µL zeocin, at 37°C and 5% $CO_{2.}$ When ~70% confluent TS-SNAP-β_2AR expression was induced with 1µg/mL tetracycline. Cells were left to express for 50hrs before harvesting.

Labelling TS-SNAP-β_2AR with Terbium cryptate

Media was aspirated from T175 flasks and adherent cells washed twice at room temperature with Phosphate Buffered Saline (PBS). Adherent cells were labelled with 100nM SNAP-Lumi4-Tb labelling reagent in Labmed buffer (both Cisbio, UK) for 1 hr at 37°C and 5% $CO_{2.}$ Cells were washed twice more with PBS and detached with 5mL non enzymatic cell dissociation solution (Sigma, UK). Cells were pelleted by centrifugation for 10 min at 1000*xg*, supernatant was removed, and cell pellets frozen at -80°C.

TS-SNAP-β_2AR membrane preparation

Cell pellets were thawed on ice and resuspended in 20mL buffer B (10mM HEPES and 10mM EDTA, pH 7.4). Suspensions were homogenised using 6 x 1 sec pulses of a Polytron tissue homogeniser (Werke, Ultra-Turrax). Suspensions were centrifuged at 48,000x*g* and 4°C for 30 min, supernatant was removed and resuspended and centrifuged again as above. Resulting pellets were resuspended in buffer C (10mM HEPES and 0.1mM EDTA, pH 7.4) and frozen at -80°C.

Solubilisation of TS-SNAP-β_2AR using DDM or DIBMA

Membranes were incubated with 3% DIBMA (w/v) (Anatrace, UK) in 20mM HEPES, 10% (v/v) glycerol, and 150mM NaCl, pH 8 at room temperature or 1% DDM (w/v), 20mM HEPES, 5% (v/v) glycerol, and 150mM NaCl, pH 8 at 4°C for 2-3 h. Samples were clarified by ultracentrifugation at 4°C for 1hr at 100,000*xg* for ligand binding assays and 16900*xg* for thermostability assays.

TR-FRET ligand binding assays

TR-FRET between the donor Lumi4-Tb and the fluorescent acceptors 633/650 S-propranolol-red (CellAura, UK) (F-propranolol) was measured by exciting at 337nm and quantifying emission at 665nm and 620nm using a PheraStar FSX (BMG Labtech)

and HTRF 337 665/620 module (BMG Labtech). Assay buffer consisted of 20mM HEPES, 5% glycerol, 150mM NaCl, and 0.5% Bovine Serum Albumin (BSA), pH8 for DDM solubilised samples 0.1% DDM was used. All binding assays used a final concentration of 1% Dimethyl sulfoxide (DMSO), assay volume of 30µL, 384 well OptiPlates (PerkinElmer, US) and 3µM cyanopindolol was used to determine non-specific binding (NSB). Receptors were added to plates last and the plates were incubated at room temperature for 45 mins prior to reading. For competition binding assays 100nM of F-propranolol was used for membrane and DDM samples and 200nM F-propranolol for DIBMA samples.

ThermoFRET thermostability assays

Solubilised Lumi4-Tb labelled β2AR was incubated with 10µM BODIPY™ FL L-Cystine dye (Molecular Probes, U.S) with or without 200nM F-propranolol or 100µM cyanopindolol, for 15 mins on ice in 20mM HEPES, 150mM NaCl, 5% glycerol, 0.5% BSA, pH8. For DDM samples 0.1% DDM was used. 20µL samples were added to each well of a 96-well PCR plate and incubated for 30 min over a temperature gradient of 20-78°C across the plate using alpha cycler 2 PCR machine (PCRmax, U.K). Samples were transferred to a 384-well proxiplate (PerkinElmer, U.S). TR-FRET between BODIPY™ FL L-Cystine dye and Lumi4-Tb was read by exciting at 337nm and reading emission at 620nm and 520nm using Pherstar FSX and 337 520/620 module (BMG Labtech). F-propranolol and fluorescent XAC (F-XAC) (CellAura, UK) binding was measured using HTRF 337 665/620 module as above.

Data analysis

TR-FRET ligand binding data

Total and NSB for F-propranolol binding to the β_2AR was fitted to one-site models in GraphPad Prism 8 according to equations 1 and 2.

$$Total\ binding = \left[\frac{Bmax * X}{(K_d + X)}\right] + [NS * X + background]$$

Equation 1

Where:
NS = slope of linear nonspecific binding
Background = Y when X is 0
Bmax = the maximum specific binding
K_d = the equilibrium dissociation constant
Y = specific binding
X= concentration of tracer

$$NSB = [NS * X + background]$$

Equation 2

Specific binding of F-propranolol to the β_2AR was fitted to the one site specific binding model in GraphPad Prism 8 according to equation 3. Final K_d values were taken as an average of K_d values from individual specific curve fits.

$$\boldsymbol{Y} = \frac{Bmax * X}{(K_d + X)}$$

Equation 3

Where:
Y = specific binding
K_d = the equilibrium dissociation constant of the labelled ligand

Equilibrium competition binding data was fitted to the One site Fit K_i model in GraphPad Prism 8 according to equation 4 and 5. Final K_i values were taken as an average of individual curve fits.

$$Y = \frac{(Top - Bottom)}{(1 + 10^{(x - LogIC_{50})}) + Bottom}$$

Equation 4

Where:
Y = binding of tracer
IC_{50} = the concentration of competing ligand which displaces 50% of radioligand specific binding.

$$K_i = \frac{IC_{50}}{1 + \left(\frac{[L]}{K_d}\right)}$$

Equation 5

Where:
K_i = the inhibition constant of the unlabelled ligand
[L] = concentration of labelled ligand
K_d = the equilibrium dissociation constant of the labelled ligand.

ThermoFRET thermostability curves
All ThermoFRET thermostability data from each experiment was fitted to a Boltzmann sigmoidal curve using GraphPad Prism 8 according to equation 6 to obtain a melting temperature (Tm) value. Final Tm values were taken as an average of Tm values from individual curve fits.

$$Y = Bottom + \frac{(Top - Bottom)}{1 + \exp\left(\frac{Tm - X}{Slope}\right)}$$

Equation 6

Where:
Y = the relative concentration of proteins in the unfolded state
X = Temperature (°C)
Tm = The temperature at which half the protein of interest is unfolded

Statistical analysis

Comparison of T_m, K_d or K_i values was made using a one-way Analysis Of Variance (ANOVA) test and Tukey's post hoc multiple comparison test. Statistical comparison of T_m values obtained with F-propranolol Vs BODIPY™ FL L-Cystine dye was made using an unpaired t test. All statistical analysis was completed in GraphPad Prism 8 and $p<0.05$ was considered statistically significant.

Supplementary information: ORF amino acid sequences for Twin-Strep-SNAP-β_2AR and Twin-Strep-SNAP-A_{2A}R

Signal peptide based on the 5HT3A receptor

Strep tag (TS)

SNAP tag

Linkers

Human β_2AR

Human A_{2A}

Amino acid sequence for Twin-Strep-SNAP-β_2AR

MRLCIPQVLLALFLSMLTGPGEGSASDIGAPAFKSVQTGEFTAAAGSAWSHPQFEKGGGSGG
GSGGSAWSHPQFEKGSGGSEDLMDKDCEMKRTTLDSPLGKLELSGCEQGLHRIIFLGKGTSA
ADAVEVPAPAAVLGGPEPLMQATAWLNAYFHQPEAIEEFPVPALHHPVFQQESFTRQVLWKL
LKVVKFGEVISYSHLAALAGNPAATAAVKTALSGNPVPILIPCHRVVQGDLDVGGYEGGLAV
KEWLLAHEGHRLGKPGLGPAGTMGQPGNGSAFLLAPNGSHAPDHDVTQQRDEVWVVGMGIVM
SLIVLAIVFGNVLVITAIAKFERLQTVTNYFITSLACADLVMGLAVVPFGAAHILMKMWTFG
NFWCEFWTSIDVLCVTASIETLCVIAVDRYFAITSPFKYQSLLTKNKARVIILMVWIVSGLT
SFLPIQMHWYRATHQEAINCYANETCCDFFTNQAYAIASSIVSFYVPLVIMVFVYSRVFQEA
KRQLQKIDKSEGRFHVQNLSQVEQDGRTGHGLRRSSKFCLKEHKALKTLGIIMGTFTLCWLP
FFIVNIVHVIQDNLIRKEVYILLNWIGYVNSGFNPLIYCRSPDFRIAFQELLCLRRSSLKAY
GNGYSSNGNTGEQSGYHVEQEKENKLLCEDLPGTEDFVGHQGTVPSDNIDSQGRNCSTNDSL
L*

Amino acid sequence for Twin-Strep-SNAP-A_{2A}

MRLCIPQVLLALFLSMLTGPGEGSASDIGAPAFKSVQTGEFTAAAGSAWSHPQFEKGGGSGG
GSGGSAWSHPQFEKGSGGSEDLMDKDCEMKRTTLDSPLGKLELSGCEQGLHRIIFLGKGTSA
ADAVEVPAPAAVLGGPEPLMQATAWLNAYFHQPEAIEEFPVPALHHPVFQQESFTRQVLWKL
LKVVKFGEVISYSHLAALAGNPAATAAVKTALSGNPVPILIPCHRVVQGDLDVGGYEGGLAV
KEWLLAHEGHRLGKPGLGPAGTPIMGSSVYITVELAIAVLAILGNVLVCWAVWLNSNLQNVT
NYFVVSLAAADIAVGVLAIPFAITISTGFCAACHGCLFIACFVLVLTQSSIFSLLAIAIDRY
IAIRIPLRYNGLVTGTRAKGIIAICWVLSFAIGLTPMLGWNNCGQPKEGKNHSQGCGEGQVA
CLFEDVVPMNYMVYFNFFACVLVPLLLMLGVYLRIFLAARRQLKQMESQPLPGERARSTLQK
EVHAAKSLAIIVGLFALCWLPLHIINCFTFFCPDCSHAPLWLMYLAIVLSHTNSVVNPFIYA
YRIREFRQTFRKIIRSHVLRQQEPFKAAGTSARVLAAHGSDGEQVSLRLNGHPPGVWANGSA
PHPERRPNGYALGLVSGGSAQESQGNTGLPDVELLSHELKGVCPEPPGLDDPLAQDGAGVS*

References

Bada Juarez, J. F., J. C. Munoz-Garcia, R. Inacio Dos Reis, A. Henry, D. McMillan, M. Kriek, M. Wood, C. Vandenplas, Z. Sands, L. Castro, R. Taylor and A. Watts (2020). "Detergent-free extraction of a functional low-expressing GPCR from a human cell line." Biochim Biophys Acta Biomembr **1862**(3): 183152.

Baker, J. G. (2005). "The selectivity of beta-adrenoceptor antagonists at the human beta1, beta2 and beta3 adrenoceptors." Br J Pharmacol **144**(3): 317-322.

Bang, I. and H. J. Choi (2015). "Structural features of beta2 adrenergic receptor: crystal structures and beyond." Mol Cells **38**(2): 105-111.

Cherezov, V., D. M. Rosenbaum, M. A. Hanson, S. G. Rasmussen, F. S. Thian, T. S. Kobilka, H. J. Choi, P. Kuhn, W. I. Weis, B. K. Kobilka and R. C. Stevens (2007). "High-resolution crystal structure of an engineered human beta2-adrenergic G protein-coupled receptor." Science **318**(5854): 1258-1265.

Comeo, E., N. D. Kindon, M. Soave, L. A. Stoddart, L. E. Kilpatrick, P. J. Scammells, S. J. Hill and B. Kellam (2020). "Subtype-Selective Fluorescent Ligands as Pharmacological Research Tools for the Human Adenosine A2A Receptor." J Med Chem **63**(5): 2656-2672.

Dawaliby, R., C. Trubbia, C. Delporte, M. Masureel, P. Van Antwerpen, B. K. Kobilka and C. Govaerts (2016). "Allosteric regulation of G protein-coupled receptor activity by phospholipids." Nat Chem Biol **12**(1): 35-39.

Dorr, J. M., M. C. Koorengevel, M. Schafer, A. V. Prokofyev, S. Scheidelaar, E. A. van der Cruijsen, T. R. Dafforn, M. Baldus and J. A. Killian (2014). "Detergent-free isolation, characterization, and functional reconstitution of a tetrameric K+ channel: the power of native nanodiscs." Proc Natl Acad Sci U S A **111**(52): 18607-18612.

Gregorio, G. G., M. Masureel, D. Hilger, D. S. Terry, M. Juette, H. Zhao, Z. Zhou, J. M. Perez-Aguilar, M. Hauge, S. Mathiasen, J. A. Javitch, H. Weinstein, B. K. Kobilka and S. C. Blanchard (2017). "Single-molecule analysis of ligand efficacy in beta2AR-G-protein activation." Nature **547**(7661): 68-73.

Gulamhussein, A. A., D. Meah, D. D. Soja, S. Fenner, Z. Saidani, A. Akram, S. Lallie, A. Mathews, C. Painter, M. K. Liddar, Z. Mohammed, L. K. Chiu, S. S. Sumar, H. Healy, N. Hussain, J. H. Patel, S. C. L. Hall, T. R. Dafforn and A. J. Rothnie (2019). "Examining the stability of membrane proteins within SMALPs." European Polymer Journal **112**: 120-125.

Gulati, S., M. Jamshad, T. J. Knowles, K. A. Morrison, R. Downing, N. Cant, R. Collins, J. B. Koenderink, R. C. Ford, M. Overduin, I. D. Kerr, T. R. Dafforn and A. J. Rothnie (2014). "Detergent-free purification of ABC (ATP-binding-cassette) transporters." Biochem J **461**(2): 269-278.

Hauser, A. S., M. M. Attwood, M. Rask-Andersen, H. B. Schioth and D. E. Gloriam (2017). "Trends in GPCR drug discovery: new agents, targets and indications." Nat Rev Drug Discov **16**(12): 829-842.

Heydenreich, F. M., T. Miljus, R. Jaussi, R. Benoit, D. Milic and D. B. Veprintsev (2017). "High-throughput mutagenesis using a two-fragment PCR approach." Sci Rep **7**(1): 6787.

Jamshad, M., J. Charlton, Y. P. Lin, S. J. Routledge, Z. Bawa, T. J. Knowles, M. Overduin, N. Dekker, T. R. Dafforn, R. M. Bill, D. R. Poyner and M. Wheatley (2015). "G-protein coupled receptor solubilization and purification for biophysical analysis and functional studies, in the total absence of detergent." Biosci Rep **35**(2).

Knowles, T. J., R. Finka, C. Smith, Y. P. Lin, T. R. Dafforn and M. Overduin (2009). "Membrane proteins solubilized intact in lipid containing nanoparticles bounded by styrene maleic acid copolymer." J Am Chem Soc **131**(22): 7458-7485.
Leitz, A. J., T. H. Bayburt, A. N. Barnakov, B. A. Springer and S. G. Sligar (2006). "Functional reconstitution of Beta2-adrenergic receptors utilizing self-assembling Nanodisc technology." Biotechniques **40**(5): 601-602, 604, 606, passim.
Manglik, A., T. H. Kim, M. Masureel, C. Altenbach, Z. Yang, D. Hilger, M. T. Lerch, T. S. Kobilka, F. S. Thian, W. L. Hubbell, R. S. Prosser and B. K. Kobilka (2015). "Structural Insights into the Dynamic Process of beta2-Adrenergic Receptor Signaling." Cell **161**(5): 1101-1111.
Mosslehy, W., N. Voskoboynikova, A. Colbasevici, A. Ricke, D. Klose, J. P. Klare, A. Y. Mulkidjanian and H. J. Steinhoff (2019). "Conformational Dynamics of Sensory Rhodopsin II in Nanolipoprotein and Styrene-Maleic Acid Lipid Particles." Photochem Photobiol **95**(5): 1195-1204.
Munk, C., E. Mutt, V. Isberg, L. F. Nikolajsen, J. M. Bibbe, T. Flock, M. A. Hanson, R. C. Stevens, X. Deupi and D. E. Gloriam (2019). "An online resource for GPCR structure determination and analysis." Nat Methods **16**(2): 151-162.
Oluwole, A. O., B. Danielczak, A. Meister, J. O. Babalola, C. Vargas and S. Keller (2017). "Solubilization of Membrane Proteins into Functional Lipid-Bilayer Nanodiscs Using a Diisobutylene/Maleic Acid Copolymer." Angew Chem Int Ed Engl **56**(7): 1919-1924.
Oluwole, A. O., J. Klingler, B. Danielczak, J. O. Babalola, C. Vargas, G. Pabst and S. Keller (2017). "Formation of Lipid-Bilayer Nanodiscs by Diisobutylene/Maleic Acid (DIBMA) Copolymer." Langmuir **33**(50): 14378-14388.
Paila, Y. D., E. Jindal, S. K. Goswami and A. Chattopadhyay (2011). "Cholesterol depletion enhances adrenergic signaling in cardiac myocytes." Biochim Biophys Acta **1808**(1): 461-465.
Rasmussen, S. G., B. T. DeVree, Y. Zou, A. C. Kruse, K. Y. Chung, T. S. Kobilka, F. S. Thian, P. S. Chae, E. Pardon, D. Calinski, J. M. Mathiesen, S. T. Shah, J. A. Lyons, M. Caffrey, S. H. Gellman, J. Steyaert, G. Skiniotis, W. I. Weis, R. K. Sunahara and B. K. Kobilka (2011). "Crystal structure of the beta2 adrenergic receptor-Gs protein complex." Nature **477**(7366): 549-555.
Routledge, S. J., M. Jamshad, H. A. Little, Y. P. Lin, J. Simms, A. Thakker, C. M. Spickett, R. M. Bill, T. R. Dafforn, D. R. Poyner and M. Wheatley (2020). "Ligand-induced conformational changes in a SMALP-encapsulated GPCR." Biochim Biophys Acta Biomembr **1862**(6): 183235.
Schioth, H. B. and R. Fredriksson (2005). "The GRAFS classification system of G-protein coupled receptors in comparative perspective." Gen Comp Endocrinol **142**(1-2): 94-101.
Stroud, Z., S. C. L. Hall and T. R. Dafforn (2018). "Purification of membrane proteins free from conventional detergents: SMA, new polymers, new opportunities and new insights." Methods **147**: 106-117.
Sun, C., S. Benlekbir, P. Venkatakrishnan, Y. Wang, S. Hong, J. Hosler, E. Tajkhorshid, J. L. Rubinstein and R. B. Gennis (2018). "Structure of the alternative complex III in a supercomplex with cytochrome oxidase." Nature **557**(7703): 123-126.
Sykes, D. A., C. Parry, J. Reilly, P. Wright, R. A. Fairhurst and S. J. Charlton (2014). "Establishing “Micro PK/PD” at the β2-Adrenoceptor." Molecular Pharmacology **85**(4): 608-617.

Wacker, D., G. Fenalti, M. A. Brown, V. Katritch, R. Abagyan, V. Cherezov and R. C. Stevens (2010). "Conserved binding mode of human beta2 adrenergic receptor inverse agonists and antagonist revealed by X-ray crystallography." J Am Chem Soc **132**(33): 11443-11445.

Whorton, M. R., M. P. Bokoch, S. G. Rasmussen, B. Huang, R. N. Zare, B. Kobilka and R. K. Sunahara (2007). "A monomeric G protein-coupled receptor isolated in a high-density lipoprotein particle efficiently activates its G protein." Proc Natl Acad Sci U S A **104**(18): 7682-7687.

Zocher, M., C. Zhang, S. G. Rasmussen, B. K. Kobilka and D. J. Muller (2012). "Cholesterol increases kinetic, energetic, and mechanical stability of the human beta2-adrenergic receptor." Proc Natl Acad Sci U S A **109**(50): E3463-3472.